Paper submittal to the ASME Journal of ElectronicP ackaging

SOLDER JOINT CREEP AND STRESS RELAXATION DEPENDENCE ON CONSTRUCTION AND ENVIRONMENTAL-STRESS PARAMETERS

R.G. Ross Jr., L.C. Wen, and G.R. Mon

Mail Stop 233-105
Jet Propulsion Laboratory
48000ak Grove Dr.
Pasadena, CA 91109
Phone (818) 354-9349
FAX (818) 393-4206

Per the journal requirements this paper has not been published elsewhere, or been submitted for publication elsewhere.

SOLDER JOINT CREEP AND STRESS RELAXATION DEPENDENCE ON CONSTRUCTION AND ENVIRONMENTAL-STRESS PARAMETERS

R.G. Ross, Jr., L.C. Wen and G.R. Mon

Jet Propulsion Laboratory
California Institute of Technology
Pasadena, California 91109

ABSTRACT

Creep strain is probably the most important time-dependent damage accrual factor affecting solder joint reliability. Under typical multi-hour loading conditions, creep-induced strain is a complex function of solder metallurgical structure, solder temperature, loading time per cycle, the applied stress, and the spring constant of the combined part/lead/board system.

The complex system level creep-fatigue interactions involved in electronic part solder joints are shown to be a strong function of the relative stiffness ratio κ, which is the ratio of the stiffness of the combined solder-lead system to the stiffness of the solder element by itself. For a leadless chip package, κ is close to unity. For a compliant leaded package, κ is typically in the 0.01 to 0.0001 range,

Important environmental stress dependencies, including the effects of operating temperature, displacement amplitude due to thermal and mechanical cycling, and cyclic frequency of loading are investigated for different levels of κ. Understanding the sensitivity of solder strain range to relative stiffness and these key environmental parameters is

important to understanding the behavior of alternative packaging concepts and to achieving robust electronic packaging designs and testing approaches,

INTRODUCTION

In most electronic packaging applications it is not a single high stress event that breaks a component solder joint; rather it is repeated or prolonged load applications that result in fatigue or creep failure of the solder, The principal strain in solder joints is caused by differential expansion between the part and its mounting environment due to changes in temperature (thermal cycles) and/or due to temperature gradients between the part and the board.

The fatigue-failure process is generally modelled by a Coffin-Manson type relationship, such as shown in Equation 1 (Manson, 1965):

$$N_f^{\beta}\Delta\epsilon = C \qquad (1)$$

where

N_f = number of cycles to failure
$\Delta\epsilon$ = cyclic plastic strain range
$\beta \approx 0.40$
$c \approx 0.80$

Equation 1 can be used for life prediction with flexible leaded parts only if the strain range ($\Delta\epsilon$) is the total plastic strain range including creep strain. This requires that the creep strain be accurately determined and added to any immediately produced plastic strain.

The function of strain relief elements -- such as the flexible metal leads of electronic components -- is to lower the differential-expansion induced loads (stresses) on the solder joints to levels well below the solder yield strength, thus significantly reducing the generation

of plastic strain.

While flexible leads invariably increase the reliability of soldered electrical connect ions, the level or amount of improvement varies widely with the specific application. This variability stems from the fact that the elastic spring properties of the leads that reduce the load also prolong the load on the solder. Prolonging the load over long time spans raises the specter of time-dependent failure mechanisms involving phenomena such as creep, Creep strain is probably the most important time-dependent damage accrual mechanism; under typical multi-hour loading conditions the solder joints of flexible leaded parts can be expected to undergo significant levels of strain due to creep of the solder in response to the applied elastic forces from the strain relief elements.

Because of creep effects, the total strain range during any given loading cycle can be a strong function of solder temperature, the loading time per cycle, the applied solder stress, and the spring constant of the combined part/lead/board system. In addition, solder metallurgical state, including solder composition, grain size and aging condition, also influence the solder creep rate.

Although extensive research in recent years has led to an increasingly mature understanding of the creep-fatigue properties of solder as an engineering material, much less headway has been made in quantifying solder creep-fatigue behavior at the electronic package systems level. The objective of the ongoing study described here is to explore and understand the complex systems-level creep-fatigue interactions involved in electronic part solder joints, and in particular to understand the key solder-joint structural configuration and environmental stress parameter dependencies. Important issues include the effects of component lead flexibility, solder joint geometry, operating temperature, strain cycling

depth, and cyclic frequency of loading. Understanding these issues is important to both achieving robust electronic packaging designs that meet the end-use requirements, and to defining and interpreting appropriate accelerated testing procedures for hardware qualification,

STUDY APPROACH

In studying the durability of solder joints, many important parameters such as dependence on component leads and interconnection geometry, cyclic frequency dependence, and temperature dependence, have been shown to be structural-system issues that are heavily intertwined with the materials properties of solder (Ross, 1991). With this premise, the approach of the present study has been to utilize a special purpose non-linear finite-element elastic-plastic-creep simulation program to study the behavior of solder joints in the context of the complete part-lead-solder-PWB system. The Jet Propulsion Laboratory (JPL) finite element program makes use of the fundamental constitutive equations that model the dependency of solder strain rate on applied stress, temperature, and metallurgical properties. This has the advantage of accurately including the stiffness and geometry of the entire part-lead-substrate system, spatial detail within the solder joint itself, as well as the measured metallurgical properties of solder,

Solder Constitutive Properties

Figures 1 and 2 summarize representative constitutive property data for the creep properties of solder as measured by Weinbel, et al, (1987), Avery and Backofen (1965), Zehr and Backofen (1968), Cline and Alden (1967), Murty (1973), and Kashyap and Murty

(1981); an excellent summary review of constitutive property data is also presented by Arrowood, et al. (1 991). Figure 1 highlights the strong sensitivity of solder strain rate to applied stress and the metallurgical condition of the solder, while Figure 2 illustrates the strong Arrhenius dependency of solder strain rate on temperature. Notice that solder exhibits three distinct strain-rate slope behaviors depending on the stress and temperature level, Regions I and III are regions of classic metal plastic deformation, whereas Region II is a so-called region of superplastic behavior. In this superplastic region the solder is able to withstand much larger levels of deformation without rupture,

Within each of the three regions Arrowood, et al. (1 991) note that the creep behavior of solder is well approximated by:

$$\dot{\epsilon} \propto \sigma^{n}\, g^{-p} \exp(-Q/kT) \propto \sigma^{n}\, g^{-p}\, \xi^{(T/10)} \qquad (2)$$

where:

ϵ	=	solder strain rate, see-l
σ	=	solder stress
n	=	creep exponent (typically n = 2 to 3)
g	=	grain size
p	=	grain size exponent (typically p = 1.6 to 2.3)
Q	=	thermal activation energy of creep
ξ	=	temperature dependence per 10 K (typically ξ = 1,5 to 2)
T	=	solder temperature (K)
k	=	Boltzmann constant

Note in Figure 1 that “as-cast” solder has been found to have extremely high creep resistance when compared to fine-grain "superplastic" solder; similarly, larger-grained “coarsened” solder, general] y the result of prolonged aging or thermal processing, has been found to be intermediate in creep resistance. With respect to the “as-cast” solder, Arrowood,

et al, (199 1) have observed that the much greater creep resistance reported for this solder may be caused by the highly banded Pb-Sn lamellae structure often encountered with slowly cooled cast solder joints. If so, this high level of creep resistance may not be relevant to rapidly-cooled electronic component solder joints, which often do not exhibit banded solder structures, In contrast to the anomalously low creep rate of “as-cast” solder, "superplastic" solder exhibits a much higher creep rate and tolerance to plastic deformation; this superplastic behavior is often associated with fine uniformly distributed grain structures similar to those found in electronic solder joints that are relatively small and have solidified rapidly from the melt. Of the three solder structures, “coarsened solder” is probably the most representative of aged solder joints in real electronics applications. The increased grain size of coarsened solder restricts creep strain and thus makes it more resistant to failure under creep loading conditions (see Murty (1973) and Kashyap and Murty (1981)). Because of the significant variability between "superplastic" solder and “coarsened” (larger-grain) solder, the properties of both are treated parametrically in this paper.

Finite Element Creep Simulation Modeling

To achieve a quantitative assessment of the complex system level creep-fatigue interactions involved in electronic part solder joints, the authors utilized a unique non-linear finite-element creep simulation computer program especially developed to directly utilize the solder constitutive properties described by Figures 1 and 2 and Equation 2 (Ross, et al., 1991 and Ross, et al., 1992); a similar program has also been developed by Pan (1991). Given the solder constitutive properties and the time history of environmental loading (e.g. part temperature vs. time) the JPL-developed program computes the resulting strain in each

element of the solder joint as a function of time. Varying the system geometry, cycle rate, thermal-cycle depth, or any of a wide variety of parameters, allows the resulting effects on solder strain history to be observed directly.

In operation, the program divides the time response of the solder joint into thousands of tiny time increments; for each time increment the solder's incremental plastic strain response is computed based on the existing stress in the solder, the solder's temperature, and the state of externally applied loads. The program starts each time increment by computing the instantaneous stress in each solder element using a special-purpose finite element elastic structural model of the complete part-lead-solder-PWB system. The forcing function for the stresses is the instantaneous geometry of the package system including previously accrued plastic deformation of the solder elements and lead deflections applied externally by thermal-cycle differential expansions or mechanical (isothermal) cycling. Following computation of the stress, the program uses constitutive equations for solder (a numerical expression of Figure 2) together with the current solder temperature to compute the plastic strain rate in each solder element, and thus the solder incremental strain during the time interval. A key feature of the program is the dynamic adjustment of the time increment to insure near-constant strain-rate during any given time increment. This is necessary to prevent strain integration errors and model instabilities caused by excessive stress relaxation during any given time interval. In general, the simulations presented in this paper involve incremental time steps ranging from 0,001 second to 1 minute, thus leading to as many as one million strain-increment solutions per simulation run. The shortest time increments are generally required during periods of elevated temperature where stress relaxation occurs rapidly.

Because of the heavy computational load presented by the algorithm, the finite

element description of the solder system is carefully simplified to preserve the important structural and geometric features of the solder system, while sacrificing non-critical spatial detail within the solder joint itself,

CREEP STRAIN DURING STRESS RELAXATION

It is clear from the constitutive relationships in Figures 1 and 2 that applied stress, solder metallurgical structure, and temperature strongly influence the strain developed in solder during an application loading condition. As previously pointed out, a key function of flexible leads is to reduce the stress on the solder and thereby to reduce the damaging accrual of solder strain. Unfortunately, a second manifestation of lead stiffness is to prolong the application of stress during periods of loading dwell. If the dwell period is sufficiently long, the elastic stress in the flexible leads will fully relax through creep of the solder joint, and no strain reduction will be realized. The time required for significant stress relaxation to occur is largely controlled by the stiffness of the part-lead-board system, which sets the initial solder stress for a fixed lead displacement and governs the rate at which the stress decreases as the solder strains. For loading conditions involving highly flexible leads, stress decreases slowly with increasing strain; this provides the conditions for the accrual of large solder strains over prolonged time periods.

Because creep strain development during stress relaxation is such an important part of solder joint performance with flexible leaded parts, it is useful to carefully examine the dynamics of simple elastic stress relaxation before proceeding to more complex cyclic loading conditions. An understanding of stress relaxation is also germane to the issue of long-term creep rupture of solder-joint systems that have accumulated built-in residual

stresses following the soldering operation. Such stress can occur due to differential expansion upon assembly cool-down following machine soldering, or due to elastic deflections applied to displace a misaligned lead during hand soldering.

Figure 3 presents a schematic representation of the elastic stress relaxation problem where the spring stiffness (K) is the effective stiffness of the combined solder-lead system; for the simple system shown in Figure 3, this effective stiffness is given by:

$$K = (1/K_L + 1/K_S)^{-1} \quad (3)$$

where

K_L	=	lead stiffness (lb/in)
K_S	=	solder stiffness = AE/L (lb/in)
L	=	solder length (in)
A	=	solder cross-sectional area (in^2)
E	=	modulus of elasticity of solder ($\approx 4 \times 10^6$ psi)

The stress relaxation problem is initiated by instantaneously elongating the outboard end of the spring by amount Ax and then holding it at this position; this applies an initial stress (σ_o = K Ax/A) to the solder, where A is the cross-sectional area of the solder. As the solder creeps under the applied stress, the spring load gradually decreases and the creep rate slows. Eventually the solder creeps the total distance Ax, and the spring load and solder stress reduce to zero.

To obtain a quantitative feel for the stress relaxation behavior of solder, it is usefu to examine two cases: one with a displacement (Ax = σ_o A/K) corresponding to an initial solder stress of σ_o = 1 ksi, and the second with a displacement (Ax = L/10) corresponding to a 10% solder strain upon complete stress relaxation. The 1 ksi initial-stress scenario represents typical conditions immediately following a large deflection that exceeds the solder yield strength; in this instance the solder starts with a stress close to the yield stress

independent of lead stiffness, The second case represents a fixed lead offset that does not exceed the solder yield strength. Note that yield stress for our purposes is the stress in Figure 1 at which the strain rate leads to near instantaneous straining (e, g. $\dot{\epsilon} > 10\text{-}2$ see-l).

Figures 4 and 5 present stress relaxation plots computed for these two cases using the authors' finite-element creep simulation computer program. The computations are based on the room-temperature solder constitutive properties of "superplastic" and "coarsened" solder as displayed in Figures 1 and 2. The results are presented parametrically as a function of spring stiffness ratio κ, where κ is the ratio of the stiffness of the combined solder-lead system (the spring in Fig. 3) to the stiffness of the solder element by itself, .e.

$$\kappa = K/K_s = KL/AE \qquad (4)$$

Because K is the effective stiffness of the combined solder-lead system as defined by Equation 3, $\kappa = 1$ corresponds to solder with no additional lead flexibility, and $\kappa = 0.1$ and 0.01 represent systems 10 and 100 times more flexible than the solder itself, respectively.

From Figure 4 it can be seen that without the addition of system flexibility the maximum stress-relaxation strain that can occur in solder by itself is a negligible 0,025%. This strain equals the initial elastic strain ($\epsilon = \sigma_o/E$) in the solder at 1 ksi, and is seen from Equation 1 to correspond to a fatigue life of tens of millions of cycles. This is important because it confirms that creep and stress relaxation are not important unless significant additional system flexibility is present,

In contrast, notice that for the same initial 1-ksi solder stress, flexible leads can result in very damaging levels of stress-relaxation strains. Making the leads more flexible clearly worsens the problem when the loading condition is a modestly-high fixed initial stress. This

is apparent by noting that the final creep strain (ϵ_f) is defined by:

$$\epsilon_f = \Delta x/L = \sigma_o A / K L = \sigma_o / \kappa E \quad (5)$$

To prevent stress-relaxation strain from nulling the effectiveness of flexible strain relief elements over multi-hour loading cycles, it is necessary to limit the maximum creep strain rate to well below 10^{-6} see-l; this corresponds to approximately a 1 % strain over a 3-hour period. From Figure 1 it can be seen that this requires that the maximum solder stress be less than 100 psi at room temperature--a small fraction of the solder yield stress.

This requirement for low initial stress (σ_o < 100 psi) is also apparent from the case of a fixed initial lead deflection as shown in Figure 5, Because Equation 5 defines a fixed relationship between initial stress (σ_o), strain displacement (ϵ_f), and lead stiffness (κ), Figure 5 is marked with the initial stress corresponding to each of the κ values. In this case only leads with a relative stiffness (κ) less than around 0.001 have low initial stress and limit stress relaxation during a typical multi-hour loading cycle. Notice also the important difference made" by the solder metallurgical properties ("superplastic" versus "coarsened" as defined in Figure 1).

By noting the similarity between Figures 4 and 5, it may be suspected that a single relationship can be used to describe both; indeed this is true, and Figure 6 provides this relationship as a so-called Master Curve for creep relaxation. With it, the creep relaxation behavior with any initial stress or spring-tip displacement can be easily determined.

STRAIN RANGE DURING ISOTHERMAL MECHANICAL CYCLING

As the next step in systematically understanding the role of lead flexibility on solder joint life, it is useful to extend the single-node solder model presented in Figure 3 by

imposing a cyclic mechanical displacement to the end of the spring instead of the fixed-displacement used in the stress-relaxation computations, Figures 7 and 8 describe the influence of lead stiffness, cyclic frequency, and solder temperature on the computed strain response to the cyclic displacement profile noted in Figure 9. Because the amplitude of the profile was chosen to correspond to a maximum solder strain of 42% during circumstances of complete stress relaxation, each of the curves in Figures 7 and 8 approaches this 42 % strain value asymptotically.

Looking first at Figure 7, it can be seen that very flexible leads with $\kappa < 0.001$ significant y reduce the generated strain range from cyclic loading. In addition, for highly flexible leads, the strain range amplitude is inversely proportional to frequency--thus proportional to dwell time; this is expected for constant applied stress (minimal stress relaxation), which causes constant creep strain rate during each half cycle. For very low frequencies, or very stiff leads, the solder creeps to its asymptotic equilibrium value; under such conditions solder strain is determined by the lead deflection and is independent of frequency.

Turning next to solder temperature effects, Figure 8, which is similar to Figure 7, provides the computed response of cyclic loading to solder temperature. The results for highly flexible leads are again predictable, and reflect a factor of 1.5 to 2.0 increase in strain range for each 10°C increase in temperature. This is in agreement with the classical creep rate dependence on temperature shown in Figure 2 and described by Kashyap and Murty (1981).

Lastly, Figure 10 describes the effect of variable loading displacement (Ax as defined in Fig. 9) on solder strain range; in this case the solder temperature is held fixed at 25°C and

cyclic frequency is held at 1 cycle per 3 hours, Note that for highly flexible leads the strain range varies approximately as the square of the deflection range (Ax), and for very stiff leads the curves asymptotically approach the linear ($\Delta\epsilon$ = Ax/L) dependency defined by an infinitely stiff lead (i.e. κ = 1). Also note that for a fixed Ax, the strain range for highly flexible leads varies approximately as the square of the relative spring stiffness (κ).

This stiffness and deflection-range dependence for highly flexible leads follows directly from the constitutive properties of solder as presented earlier in Equation 2. For the case of minimal stress relaxation (i.e., constant stress during each loading half cycle), the strain rate $\dot{\epsilon}$ is approximately constant; thus the total strain range for each cycle is

$$\Delta\epsilon = 2 \int \dot{\epsilon}\, dt = 2\, \dot{\epsilon}\, \tau \qquad (6)$$

where (τ) is the half-cycle dwell time. Combining Equation 6 with the constitutive properties defined by Equation 2 gives

$$\Delta\epsilon \propto \tau\, \sigma^n\, g^{-p}\, \xi^{(T/10)} \qquad (7)$$

where

σ	=	solder stress
n	=	creep exponent (typically n = 2 to 3)
g	=	grain size
p	=	grain size exponent (typically p = 1,6 to 2.3)
ξ	=	temperature dependence per 10”C (typically ξ = 1.5 to 2)
T	=	solder temperature (ºC)
τ	=	half-cycle dwell time

Noting that the solder stress is determined by σ = K Ax/A gives

$$\Delta\epsilon \propto \frac{\tau\, K\text{“ } Ax^n}{A^n\, g^p}\, \xi^{(T/10)} \qquad (8)$$

where (A) is the cross-sectional area of the solder under load. This expression for very

flexible leads notes that the strain range is proportional to roughly the square of the lead stiffness, the square of the lead displacement, and the inverse square of the grain size as defined by the values of n and p associated with Figure 1 and Equation 8. This agrees with, and provides physical insight into the numerical simulation results presented in Figure 10. For the limiting case of an infinitely rigid lead with no creep, Equation 8 reduces to $\Delta\epsilon \propto \Delta x$.

The important implication of Equation **8 is** that, for very flexible leads, the dependency of the strain range on operational parameters is fundamentally determined by the constitutive properties of solder and is very different from the parameter dependency associated with rigid leads. If these constitutive properties change for different solder types or aging conditions, then the power-law dependencies of flexible leads will also change.

COMPLEX STRAIN BEHAVIOR WITH LEADED PARTS

The preceding discussion has highlighted the important parameters influencing the development of creep strain in elastically loaded solder joints. Because creep rate is strongly dependent on the applied stress, flexible leads that lower the stress can greatly diminish the developed strain. However, with flexible leaded parts, such as a gull-wing flat-pak shown in Figure 11, the solder is subjected to a much more complex loading environment than the previously discussed single node model. There are three principal contributors to this increased complexity:

1) The solder joint is spatially distributed and attached to the part lead at multiple locations. For clarity, it is often useful to consider the joint as made up of numerous independent solder elements attached in parallel between the part lead and the

substrate.

2) The complex lead geometry causes the individual solder elements to be loaded by different stress levels in different directions. This causes some solder elements to be primarily loaded normal to the board in tension-compression, while others are primarily loaded parallel to the board in shear. The lead itself undergoes complex motion containing rotation as well as translation,

3) Because the lead is flexible, the load on the individual solder elements is highly interactive and often timewise out of phase. For example, on a gull-wing lead, the solder attaching the toe of the lead cannot be significantly loaded until the heel has deflected (see Fig. 11 for heel-toe nomenclature). This flexible coupling between the heel and toe causes a phase shift (time shift) between when the heel and toe undergo maximum straining. This is important because it implies that there is no single point in time when each element of the solder is at its maximum strain level; thus no single snap-shot in time can be used to evaluate the strain range ongoing in different elements of the solder joint.

One of the only practical means of analyzing solder joints with flexible leads is the non-linear finite element creep simulation model discussed earlier. Figure 14 illustrates the solder strain response computed for a flat-pak part using the model shown in Fig. 12 and the lead deflection profile shown in Figure 13; the lead deflection is the deflection imparted by the part/lead/board differential expansion and is noted with sign as +X in Fig. 12. The cyclic lead defection in Fig. 13 (i- 0.0003 inches) is the same magnitude as would be seen by a ceramic chip mounted to an FR-4 board and cycled between -35 and + 10WC.

The results presented in Figure 14 correspond to a gull-wing lead with a 20-mil height, a constant 32.5°C operating temperature, and a three-hour loading cycle. The structure of the finite-element model implicitly accounts for the important geometry and distributed flexibility of the lead, and the distributed nature of the solder joint.

In the results shown in Figure 14, the heel and toe rock up and down applying normal-to-the-board tension and compression to the solder. Note that the heel and toe strains are out of phase with respect to one another, and are substantially different in amplitude. Although some asymmetry occurs at the start of loading, the strain eventually becomes symmetrical about the zero-strain axis.

Figure 15 expands on the results of Figure 14 by describing the dependence of the gull-wing solder strain range on lead height, for the same 3-hour cycle and lead-deflection profile shown in Figure 13. Notice that horizontal shear strain, which is negligible with the taller lead heights, becomes dominant when the lead height is reduced below 20 roils, Notice also that the strain at the toe decreases much more rapidly with increasing lead flexibility than does the strain at the heel. These results graphically illustrate the complex inter-dependency between shear strain and heel-toe tension-compression strain with gull-wing or J-lead type leads. This interdependency reflects the fact that the effective stiffness ratio in the horizontal shear direction drops off much faster with increasing lead height than does the effective stiffness ratio in the normal-to-the-board tension-compression direction, This complex strain interdependency becomes even more important in thermal-cycling environments as discussed by Ross, et al. (1992).

Because of these complex lead stiffness interdependencies, it is instructive to revisit the sensitivity of strain range to lead deflection range Ax, solder temperature, and cyclic

frequency noted in the last section for a single node solder joint. Figure 16 combines the effects of solder temperature, lead stiffness and peak-to-peak lead deflection range into a single plot. Notice that the 20-mil flat-pak lead is quite stiff in that it exhibits little strain range reduction, near linear strain dependency on Ax, and very little temperature dependency. This is indicative of near complete creep relaxation. In contrast, the Quad-pak with much more flexible fine-pitch leads significantly reduces the strain range; as a consequence, it exhibits the strong (Ax^n) strain dependency and Arrhenius temperature dependency of creep rate noted in Figures 1 and 2 and Equation 8.

Lastly, Figure 17 displays the computed dependence of strain range on loading frequency for gull-wing leads with a constant $\pm$ 0.0003" lead deflection amplitude (per Figure 13) and 32. 5°C solder temperature. Notice that the frequency dependence of the more highly flexible fine-pitch quad-pak lead is very similar to the I/frequency dependence previously noted in Figure 7 and Equation 8. In contrast, the 20-mil flat-pak lead is seen to exhibit a significantly lower frequency dependence consistent with its higher stiffness,

DISCUSSION AND CONCLUDING SUMMARY

It has been shown that the use of highly flexible leads can greatly reduce the creep strain developed in solder joints exposed to cyclic loading conditions with multi-hour loading dwells; these environments are common for electronic assemblies that are power cycled daily (cars, computers, TVs). The key requirement is to limit the maximum solder stress to a level significantly below the solder yield stress. Depending on the lead deflection applied by the part-board system, lead stiffnesses must generally be at least 1000 times more flexible than the solder itself (i.e. $\kappa < 10^{-3}$, as defined in Equation 4).

The rate at which solder creeps is a strong function of not only the applied stress, but also the solder temperature and metallurgical structure. Temperature and solder aging conditions have been shown to have order-of-magnitude influences on creep-strain generation. The parametric studies presented provide an overview of the expected sensitivities to cycle rate, temperature, lead stiffness and strain-cycle depth. When complex lead geometries such as gull-wing leads are used, the failure location can be strongly dependent on the lead flexibility, For highly compliant leads, solder-joint failure is generally caused by tension-compression cyclic fatigue at the heel. However, for a very stiff lead, the dominant damage mechanism can be cyclic shear fatigue, When thermal cycling is introduced, even more complex behavior results from the strong creep-rate dependency on temperature. This topic is not covered in this paper, but is described by Ross, et al, (1992).

With properly designed flexible lead systems, solder strains will be substantially lower than with leadless devices, and completed boards should be capable of surviving hundreds of deep cyclic loads.

ACKNOWLEDGEMENT

The work described in this paper was carried out by the Jet Propulsion Laboratory, California Institute of Technology, under contract with the National Aeronautics and Space Administration. The authors would like to especially thank Ms. Elizabeth Jetter who conducted many of the computer simulations and generated most of the figures used in this chapter.

REFERENCES

Arrowood, R., Mukherjee, A. and Jones, W. B., 1991, "Hot Deformation of Two-phase Mixtures", Solder Mechanics: AStateof the Art Assessment, Minerals, Metals and Materials Society, Warrendale PA, 1991, pp. 107-153.

Avery, D.H. and Backofen, W. A., 1965, "A Structural Basis for Super-plasticity," Transactions of the ASM, Vol. 58, pp. 551-562.

Cline, H. E. and Alden, T. H., 1967, "Rate Sensitive Deformation in Tin-Lead Alloy," Trans. AIME, Vol. 239, pp. 710-714.

Frear, D. R., Jones, W.B. and Kinsman, K. R., 1991, Solder Mechanics: A State of the Art Assessment, Minerals, Metals and Materials Society, Warrendale PA.

Guo, Z., Sprecher, A.F. and Conrad, H ., 1991, "Plastic Deformation Kinetics of Eutectic Pb-Sn Solder Joints in Monotonic Loading and Low-cycle Fatigue", ASME Journal of Electronic Packaging, Vol. 114, No. 2, June 1992, pp. 112-117.

Kashyap, B.P. and Murty, G. S,, 1981, "Experimental Constitutive Relations for the High Temperature Deformation of a Pb-Sn Eutectic Alloy", Materials Science and Engrg, Vol. 50, pp. 205-213.

Lampe, B. T., 1976, "Room Temperature Aging Properties of Some Solder Alloys", Welding Research Supplement, October 1976, pp. 330-340.

Lau, J. H., 1991, Solder Joint Reliability: Theory and Application, Van Nostrand Reinhold, New York.

Manson, S .S., 1965, "Fatigue: A Complex Subject-- Some Simple Approximations, " Engineering Mechanics, Vol. 5, pp. 193-226.

Murty, G. S., 1973, "Stress Relaxation in SuperPlastic Materials", J. of Material Science, Vol. 8, pp. 611-614.

Pan, T-Y,, 1991, "Thermal Cycling Induced Plastic Deformation in Solder Joints--Part 1: Accumulated Deformation in Surface Mount Joints", ASME Journal of Electronic Packaging, Vol. 113, March 1991, pp. 8-15.

Ross, R. G., Jr., et al., 1992, "Solder Creep-Fatigue Interactions with Flexible Leaded Parts", ASME Journal of Electronic Packaging, Vol. 114, No. 2, June 1992, pp. 185-192.

Ross, R. G., Jr., et al., 1991, "Creep-Fatigue Behavior of Micro-electronic Solder Joints", Proceedings of the 1991 MRS Spring Meeting, Anaheim CA, April 30- May 4, 1991,

Weinbel, R. C., Tien, J. K., Pollak, R. A., and Kang, S. K., 1987, "Creep-Fatigue Interaction in Eutectic Lead-Tin Solder Alloy", J, of Material Science Letter, Vol. 6, pp. 3091-3096.

Zehr, S. W. and Backofen, W .A., 1968, "SuperPlasticity in Lead-Tin Alloys", Transaction of the ASM, Vol. 61, pp. 300-312.

FIGURE CAPTIONS

Fig. 1. Dependence of strain-rate on applied stress and metallurgical condition of room-temperature eutectic Sn-Pb solder.

Fig. 2. Dependence of strain-rate on applied stress and temperature for eutectic Sn-Pb solder (from Cline and Alden, 1967).

Fig. 3. Schematic of single-node solder element with series spring representing the combined elastic flexibility of the solder and electronic component lead,

Fig. 4. Creep-relaxation response of solder as a function of relative spring stiffness (κ) for a fixed initial loading stress of 1 ksi.

Fig. 5. Creep-relaxation response of solder as a function of relative spring stiffness (κ) for a fixed spring-tip displacement (Ax) corresponding to a 10% strain upon complete stress relaxation.

Fig. 6. Creep-relaxation Master Curves that describe creep-relaxation response of solder as a function of relative spring stiffness (κ) for initial stress (σ_o) or a spring-tip displacement (AX) corres-pending to a final strain (ϵ_f) upon complete stress relaxation.

Fig, 7. Effect of cyclic frequency of loading and relative spring stiffness (κ) on computed solder strain range.

Fig. 8. Effect of solder temperature and relative spring stiffness (κ) on computed solder strain range.

Fig. 9. Cyclic displacement profile (AX versus time) used for isothermal strain studies with single-node spring-loaded solder element.

Fig. 10. Effect of input displacement amplitude (AX) and relative spring stiffness (κ) on solder cyclic strain range ($\Delta\epsilon$).

Fig. 11. Solder-joint nomenclature and dimension definitions for flat-pak parts mounted with gull-wing leads.

Fig. 1. Dependence of strain-rate on applied stress and metallurgical condition of room-temperature eutectic Sn-Pb solder.

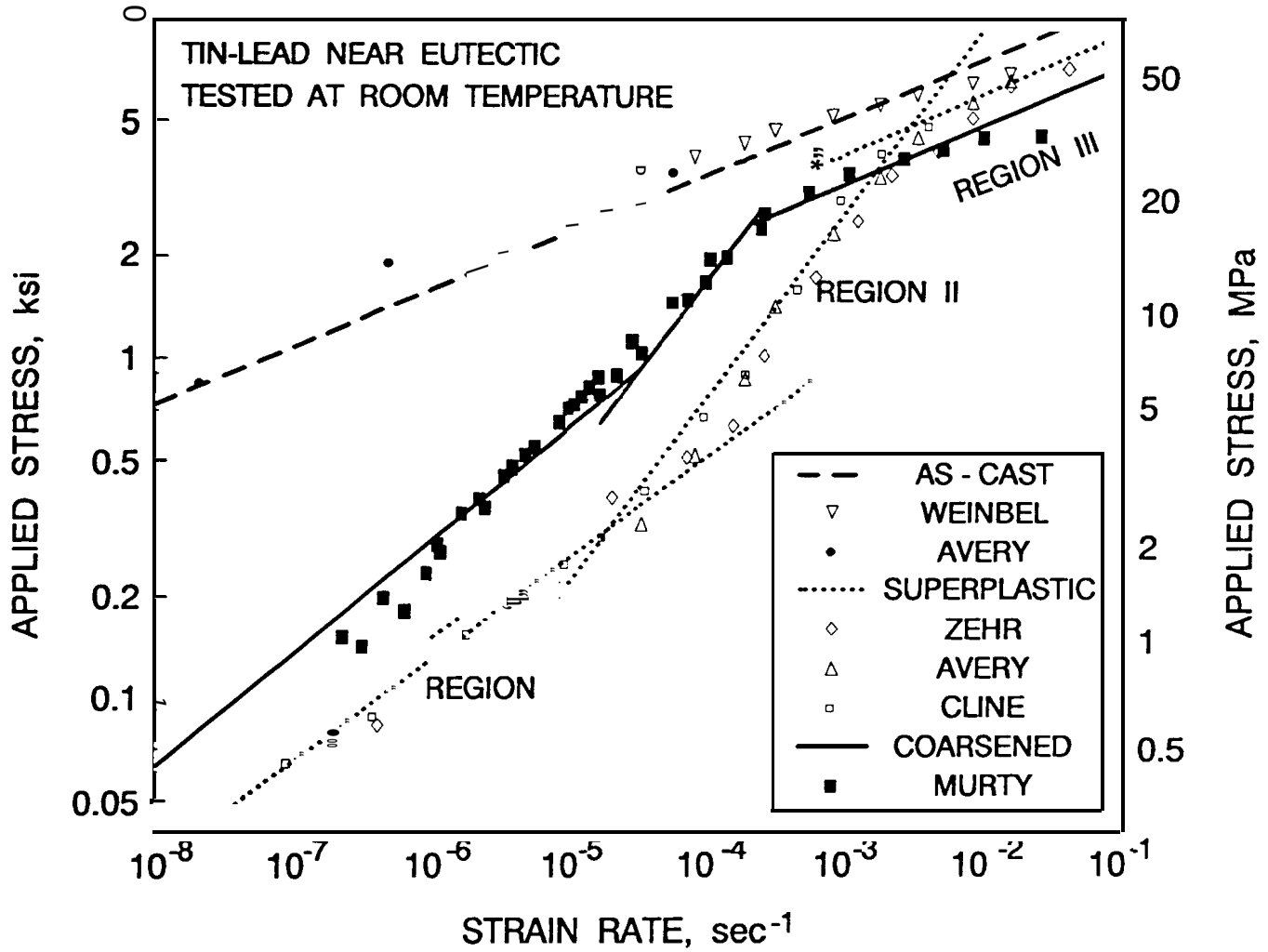

SOD_002

Fig. 2. Dependence of strain-rate on applied stress and temperature for eutectic Sn-Pb solder (from Cline and Alden, 1967).

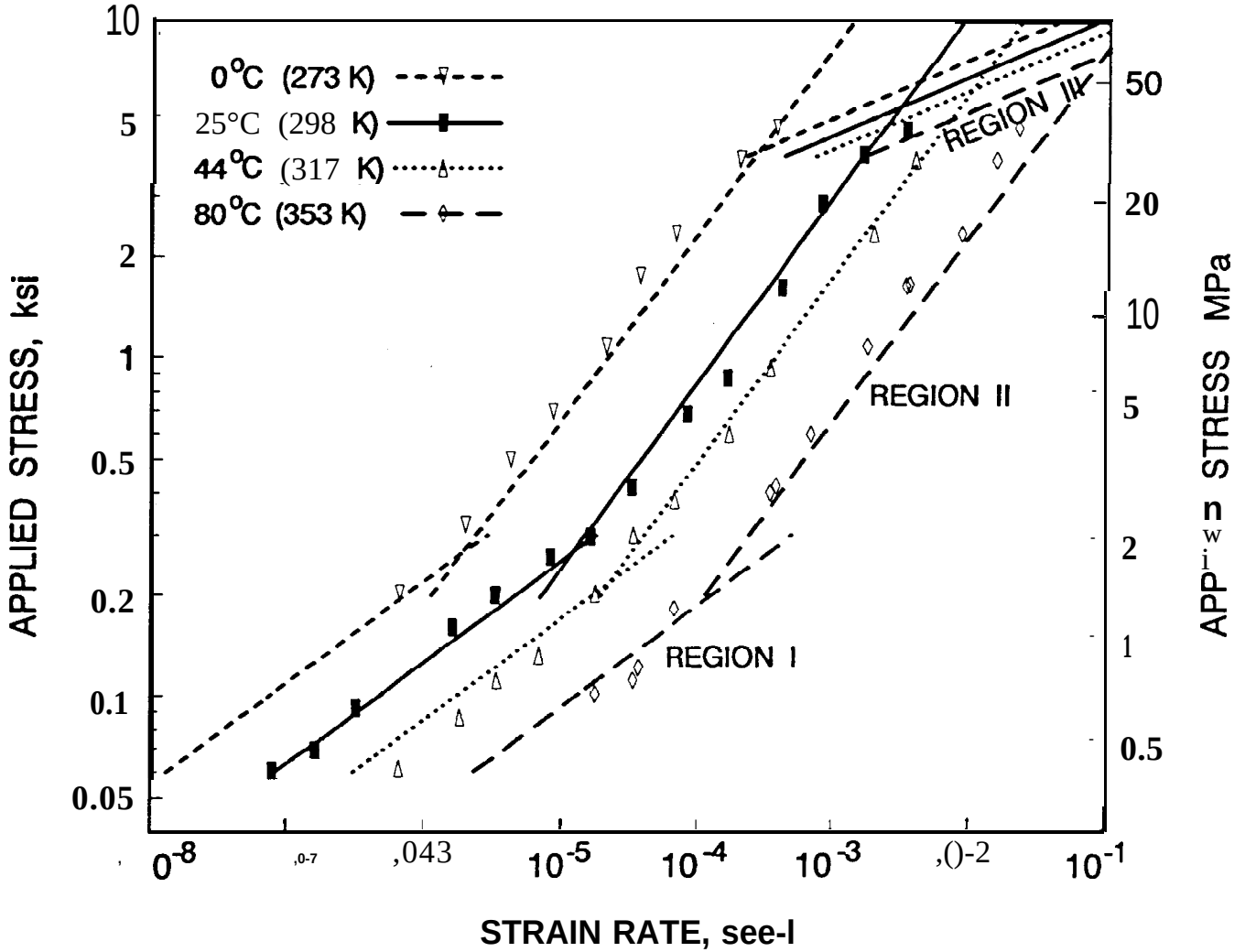

SOD_003B

Fig. 3. Schematic of single-node solder element with series spring representing the combined elastic flexibility of the solder and electronic component lead.

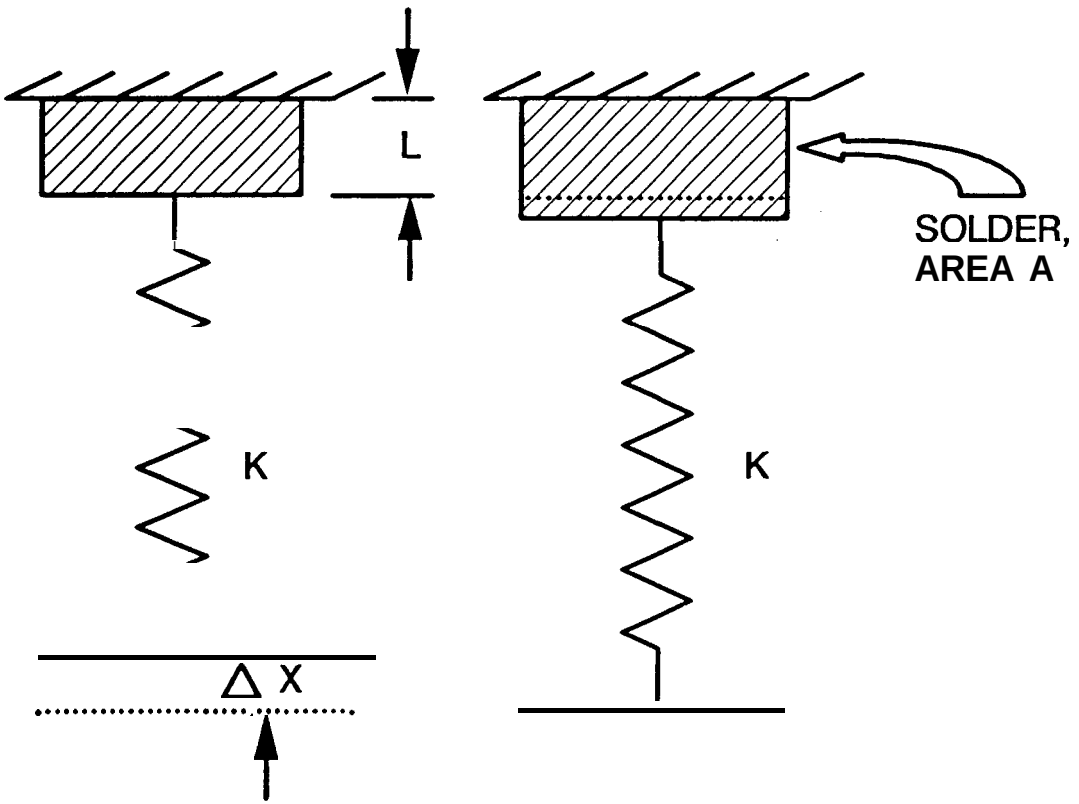

Fig. 4. Creep-relaxation response of solder as a function of relative spring stiffness (κ) for a fixed initial loading stress of 1 ksi.

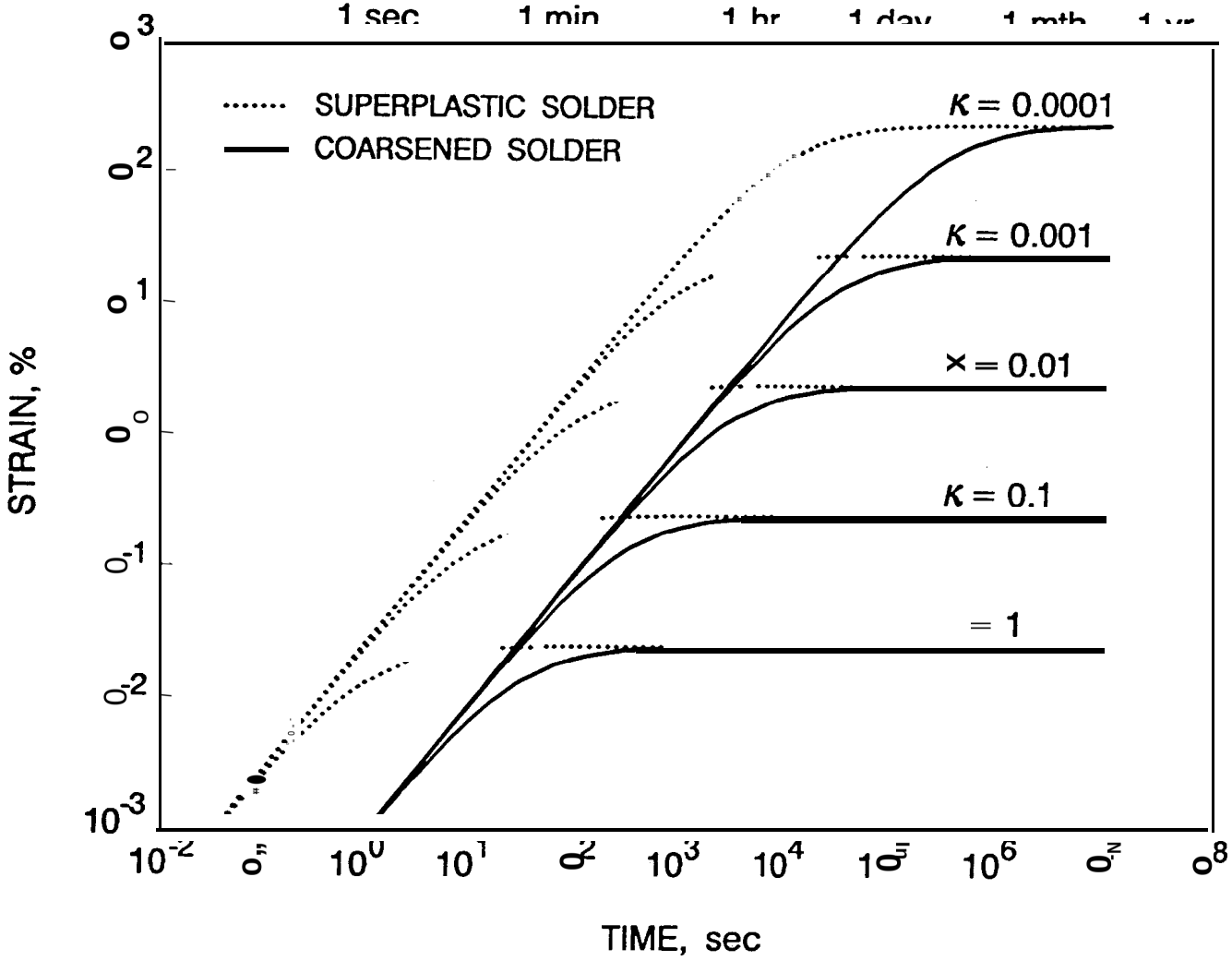

SOD_031

Fig. 5. Creep-reIaxation response of solder as a function of relative spring stiffness (K) for a fixed spring-tip displacement (Ax) corresponding to a 10% strain upon complete stress relaxation.

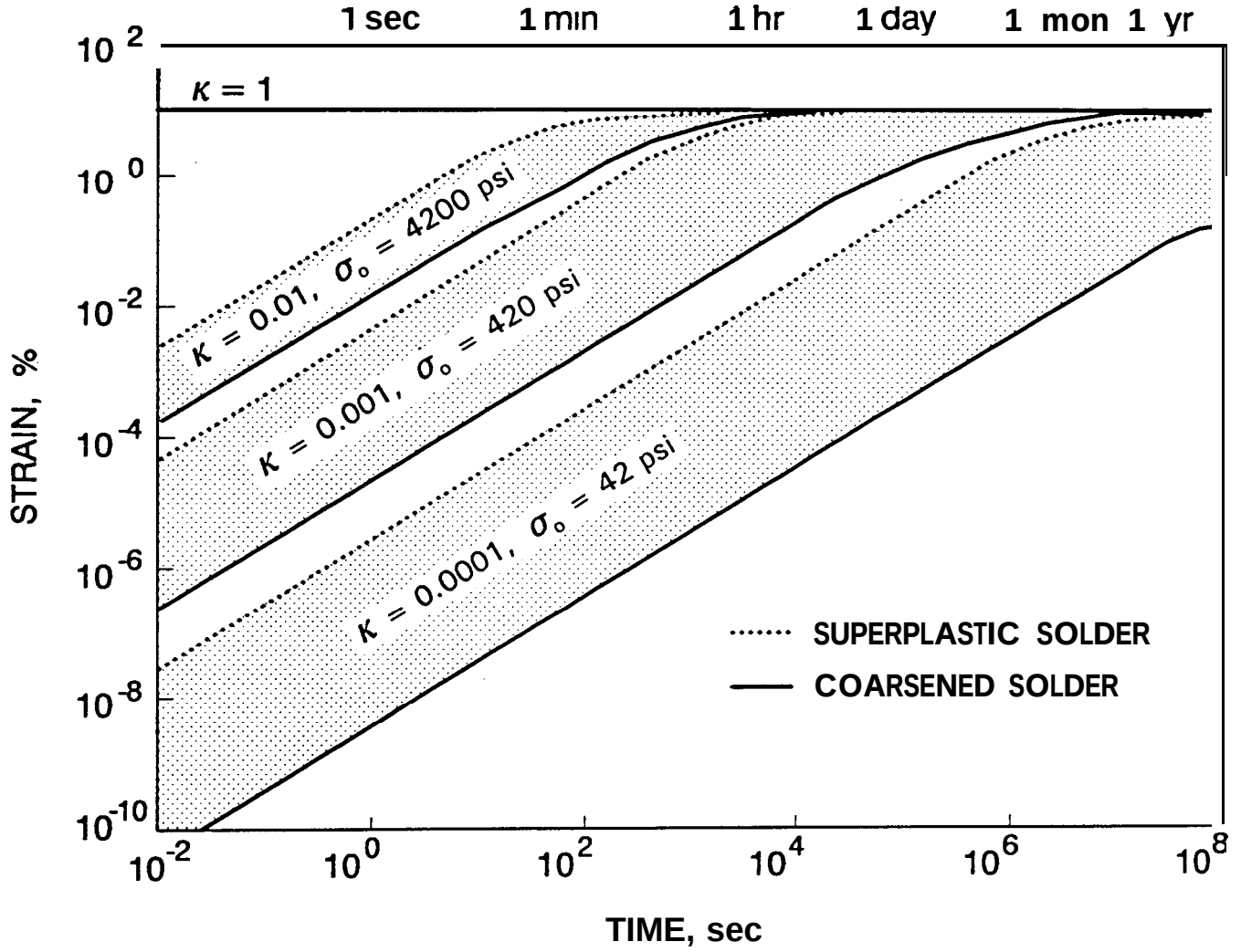

SOD_032

Fig. 6. Creep-relaxation Master Curves that describe creep-relaxation response of solder as a function of relative spring stiffness (K) for initial stress (σ_o) or a spring-tip displacement (Ax) corres-pending to a final strain (ϵ_f) upon complete stress relaxation.

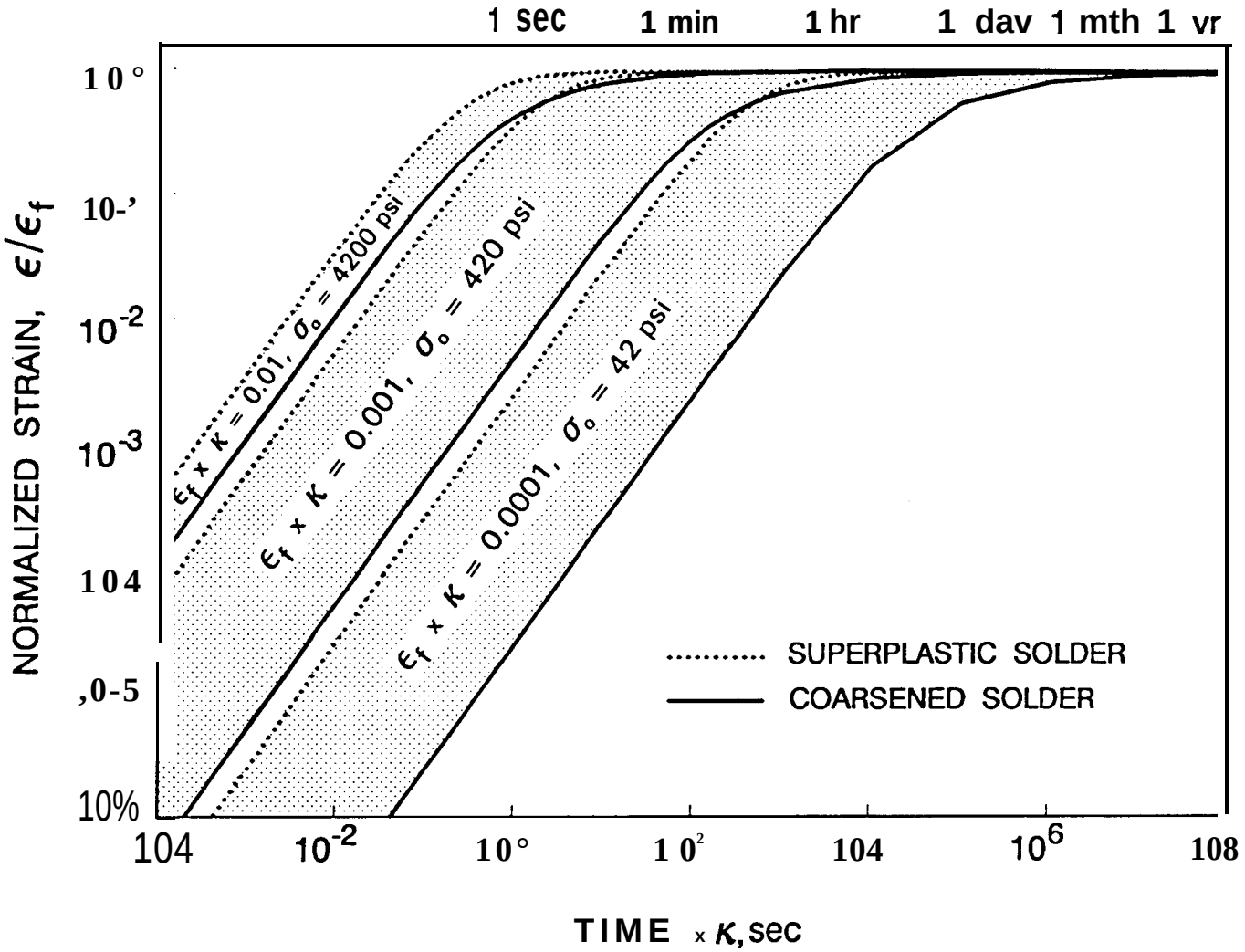

Fig. 7 Effect of cyclic frequency of loading and relative spring stiffness (κ) on m solder strain range.

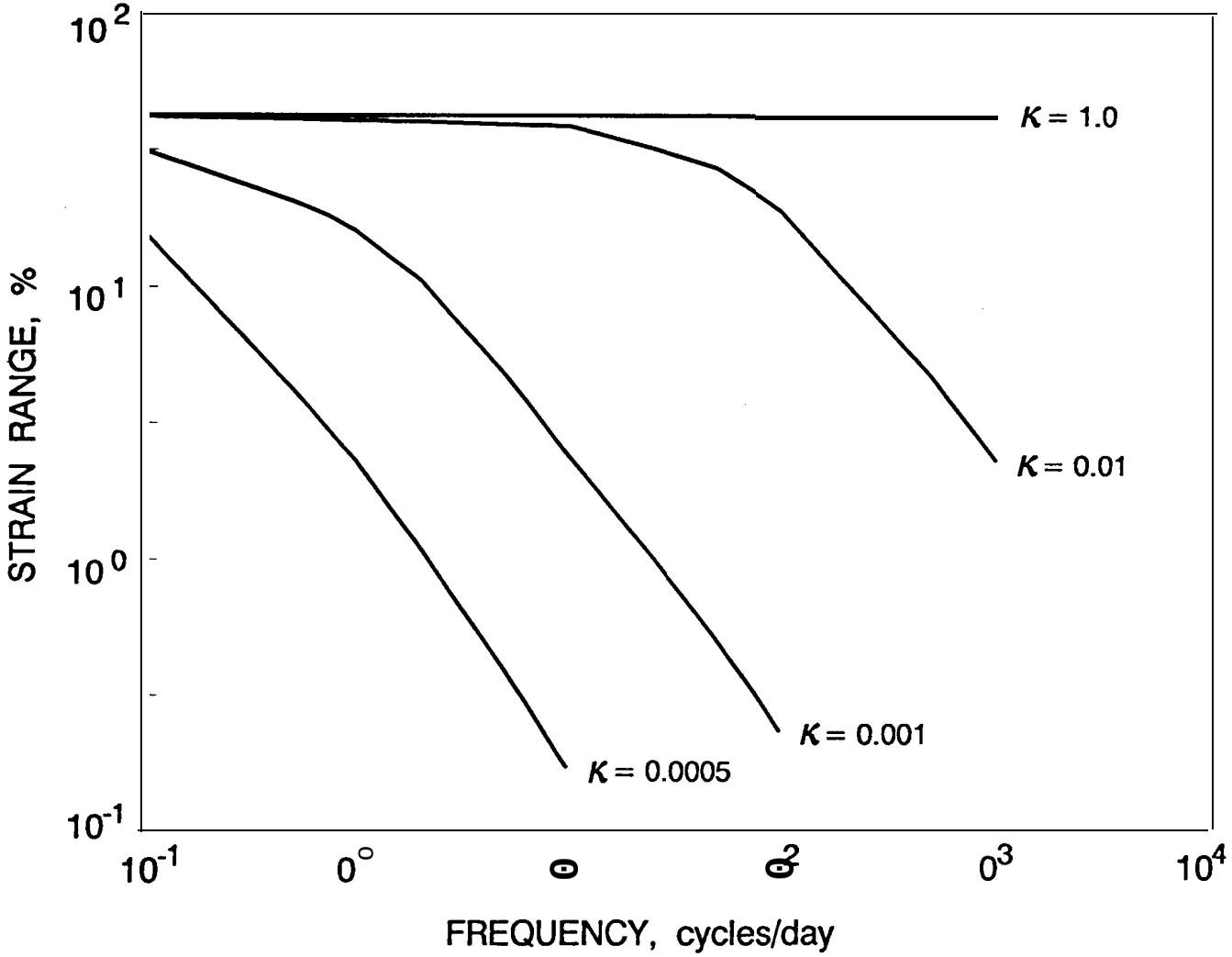

Fig. 8. Effect of solder temperature and relative spring stiffness (κ) on computed solder strain range.

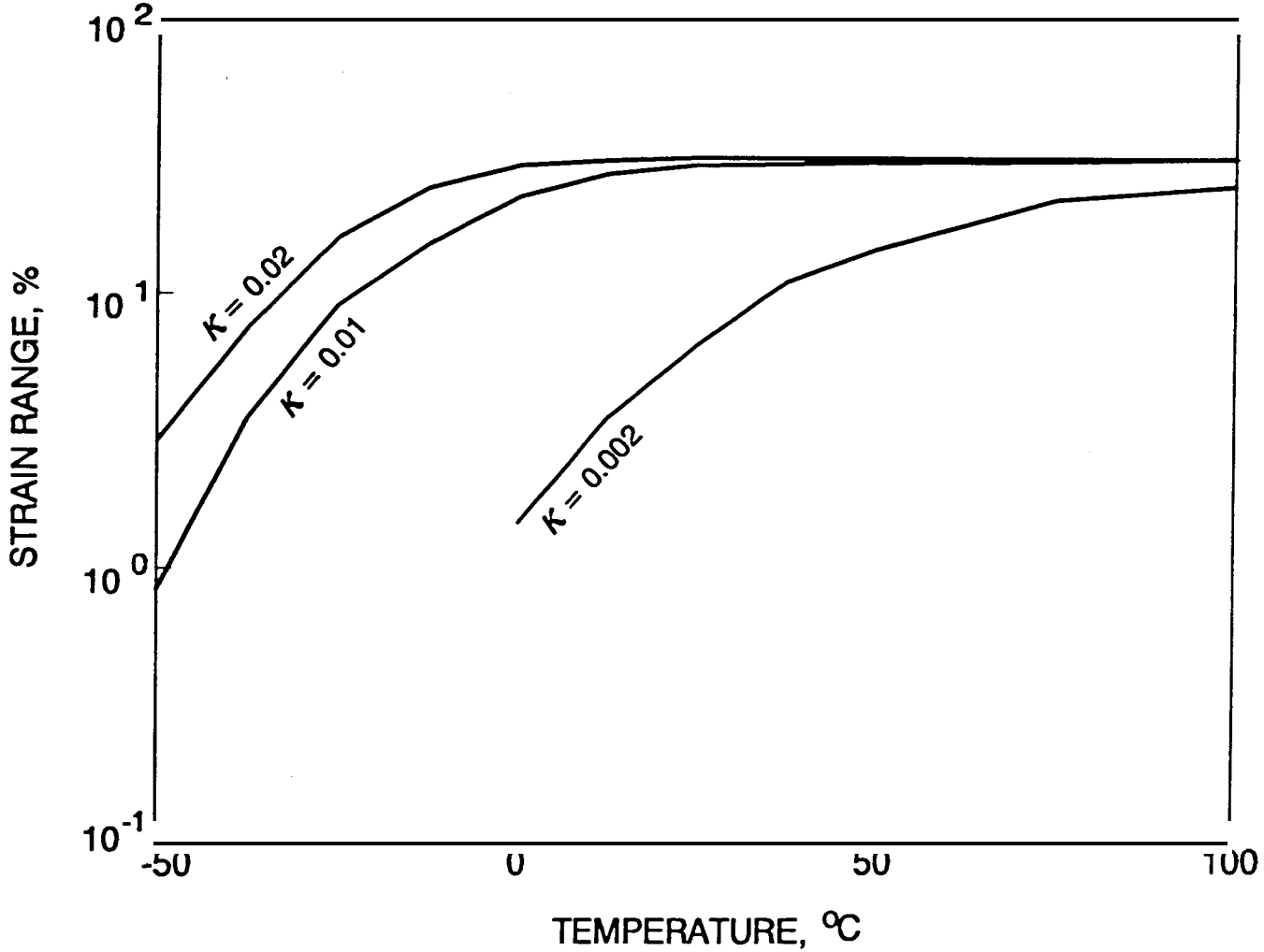

E:\WKSMOD\Fig3-6A.WK3

SO 035

Fig. 9. Cyclic displacement profile (Δx versus time) used for isothermal strain studies with single-node spring-loaded solder element.

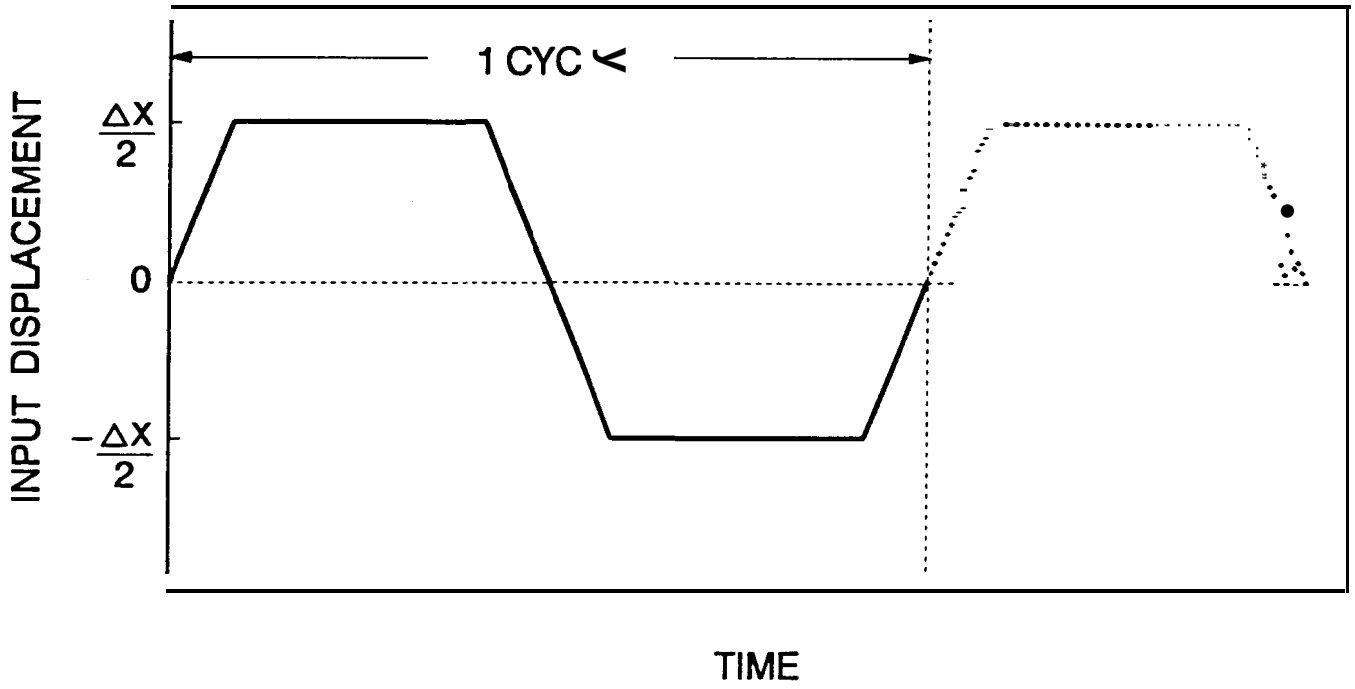

Fig. 10. Effect of input displacement amplitude (Ax) and relative spring stiffness (κ) on solder cyclic strain range (At).

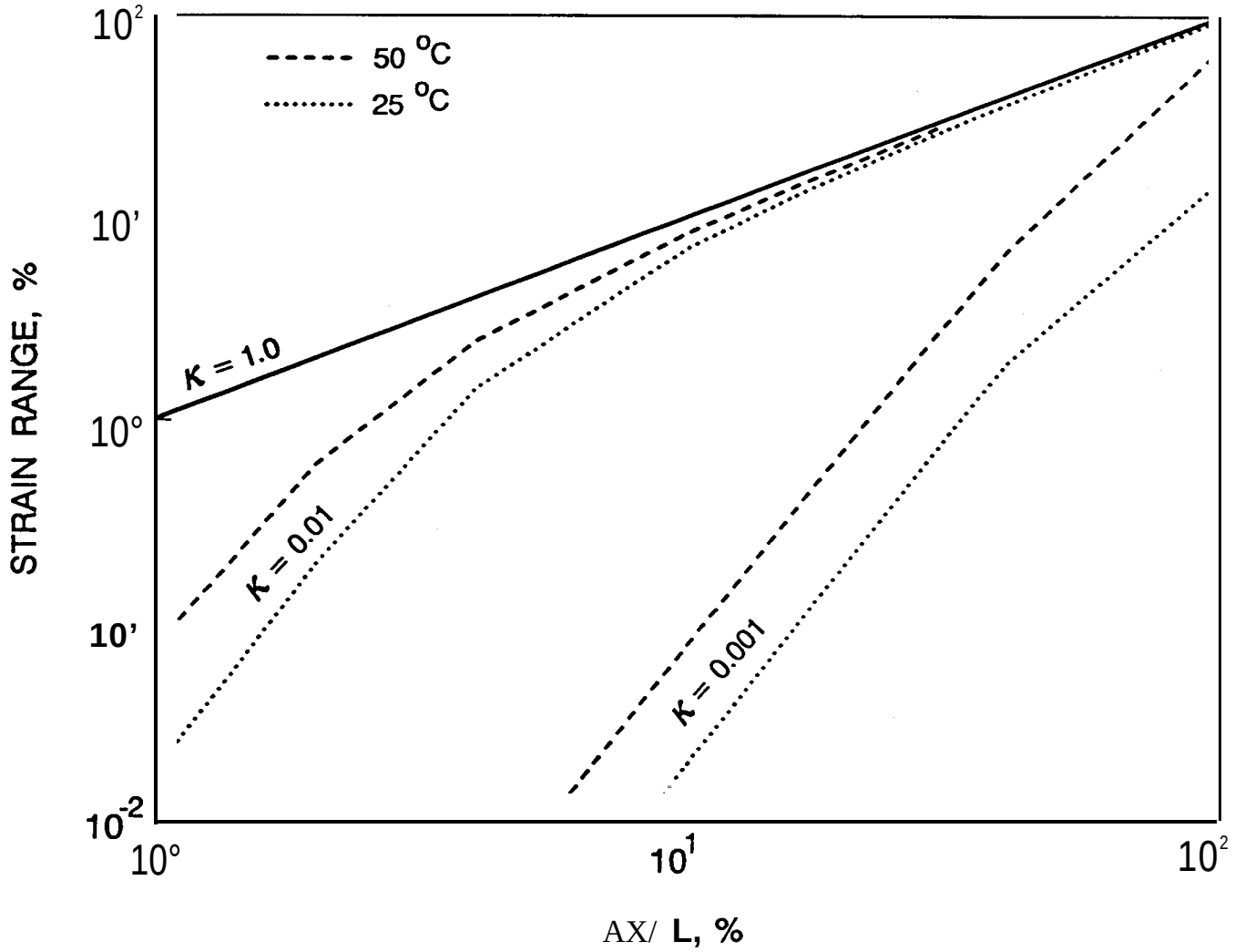

E:\WKSMOD\FIG3-8.WK3

SOD_037

Fig. 11. Solder-joint nomenclature and dimension definitions for flat-pak parts mounted with gull-wing leads.

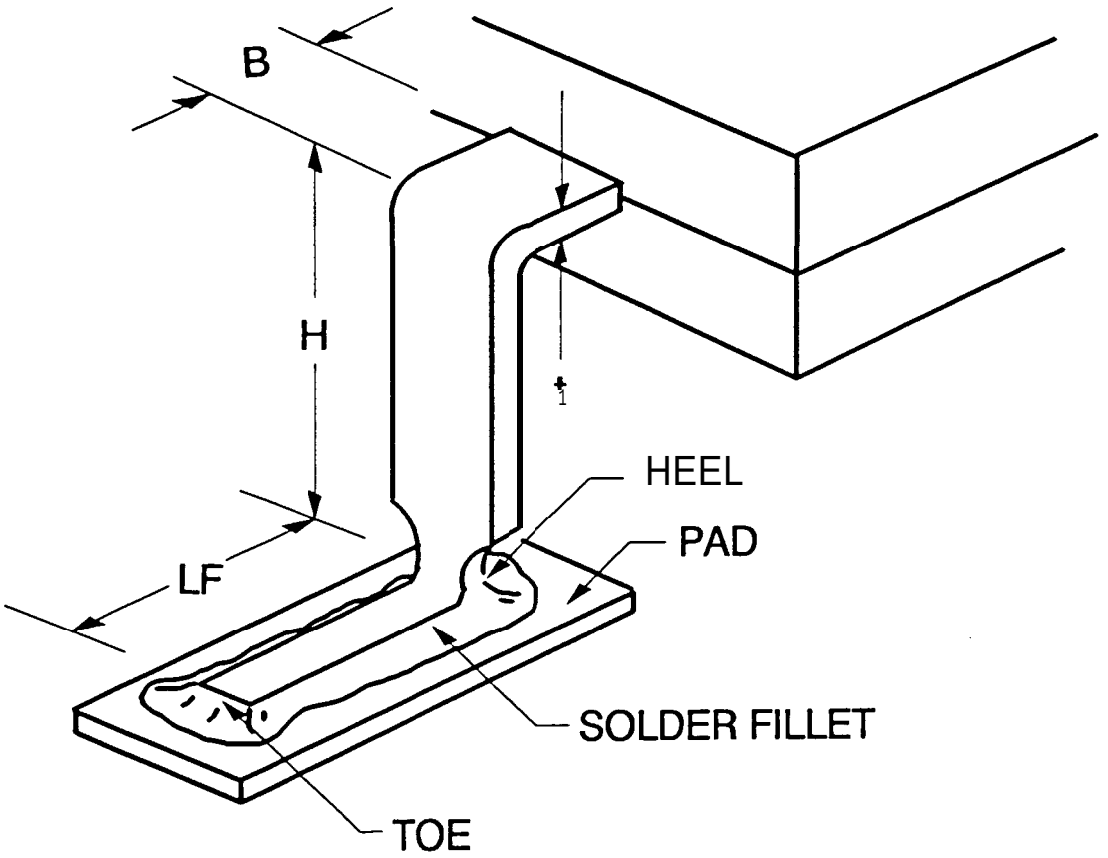

SOD_004A

Fig. 12. Schematic of finite element elastic-plastic-creep model of solder joint with gull-wing lead.

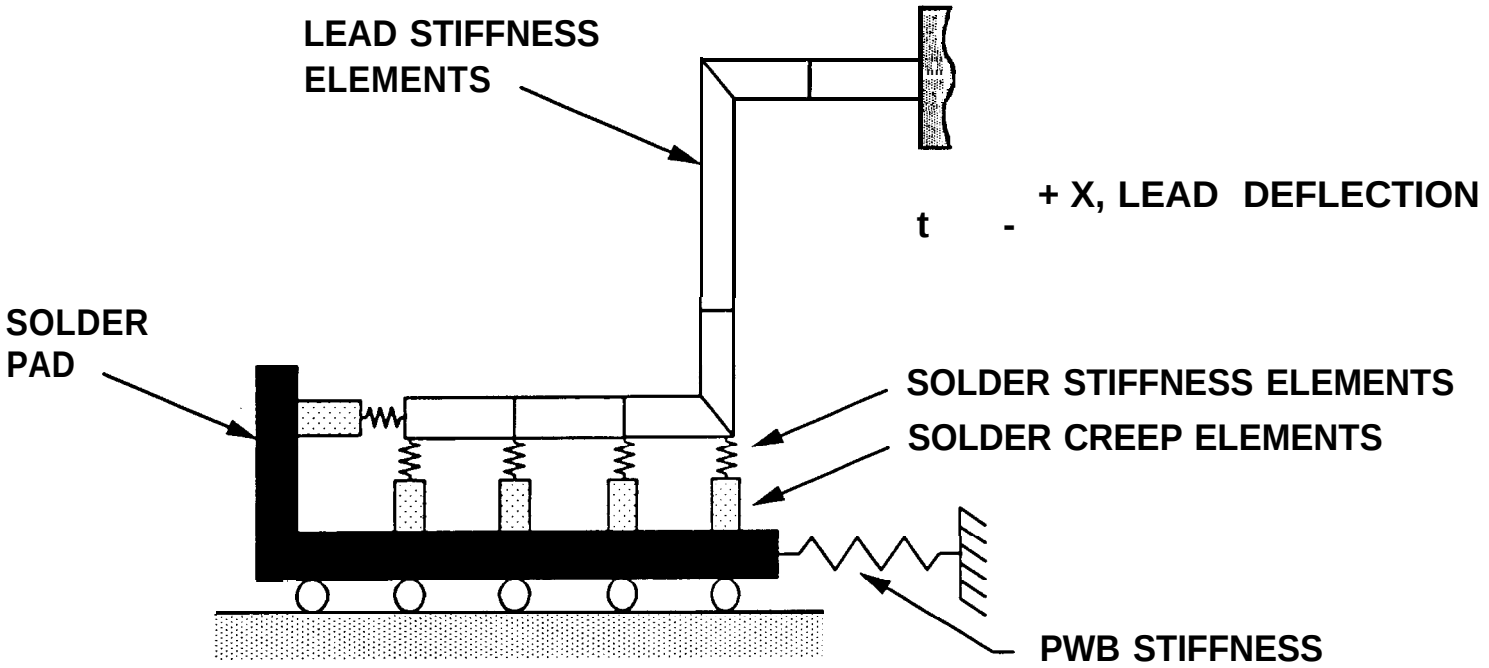

SOD_014

Fig. 3. Cyclic displacement profile (Δx versus time) used for isothermal strain response studies with gull-wing flat-pak.

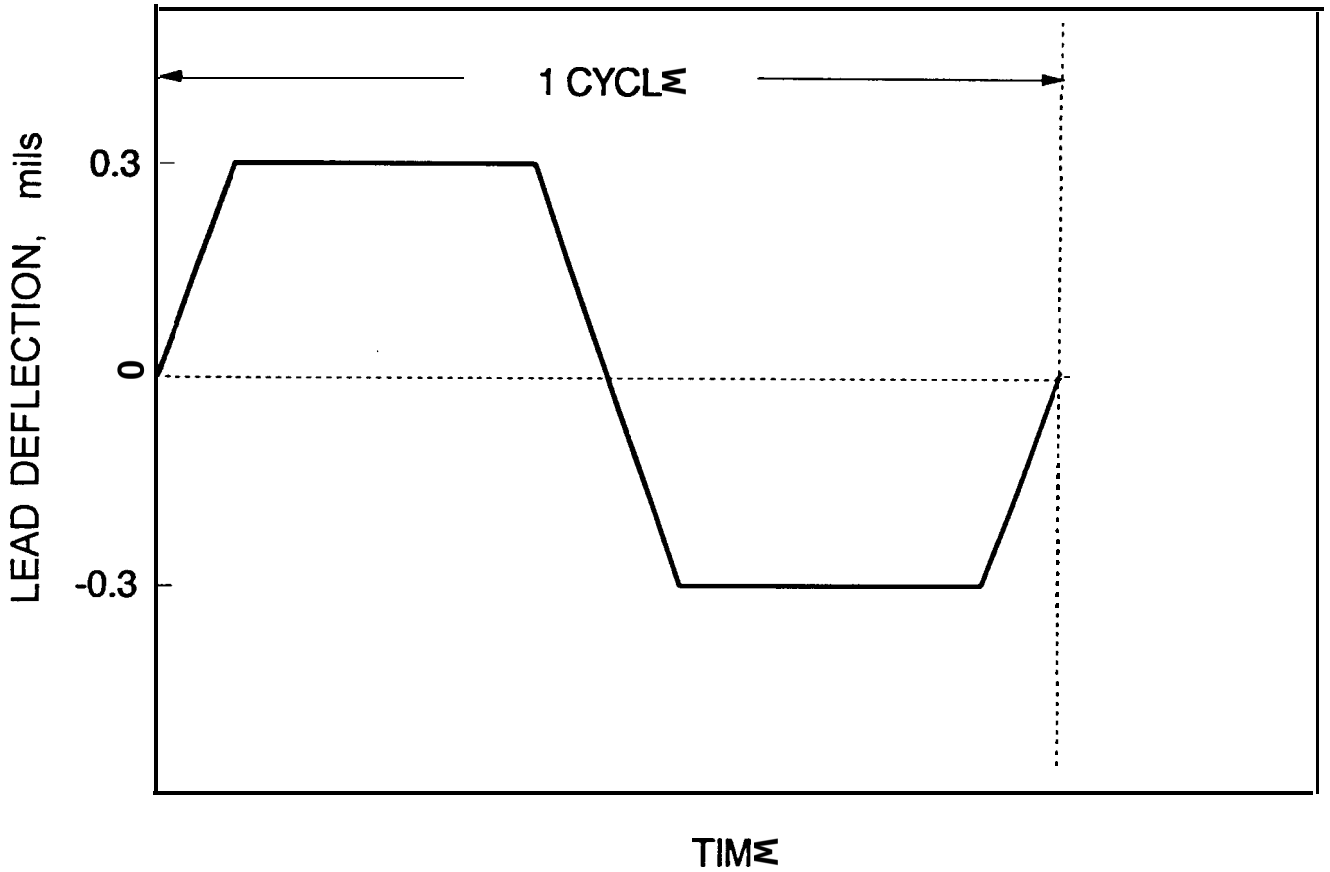

Fig. 14. Typical heel, toe and shear strain response of mechanically cycled gull-wing lead (20-mil high flat-pak).

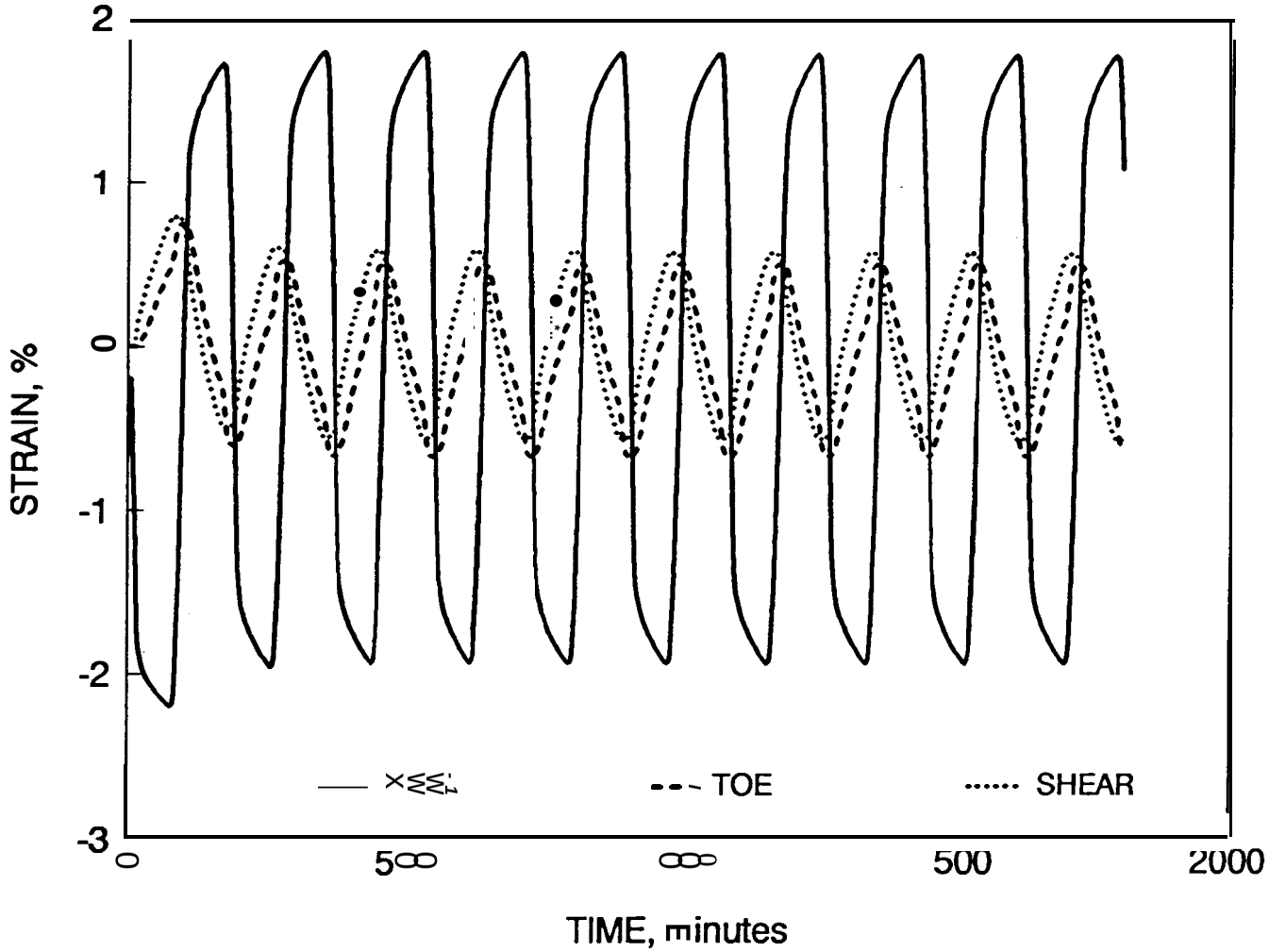

PLOTF330

SO 039

Fig. 15. Computed dependence of strain range on lead height for flat-pak parts with gull-wing leads.

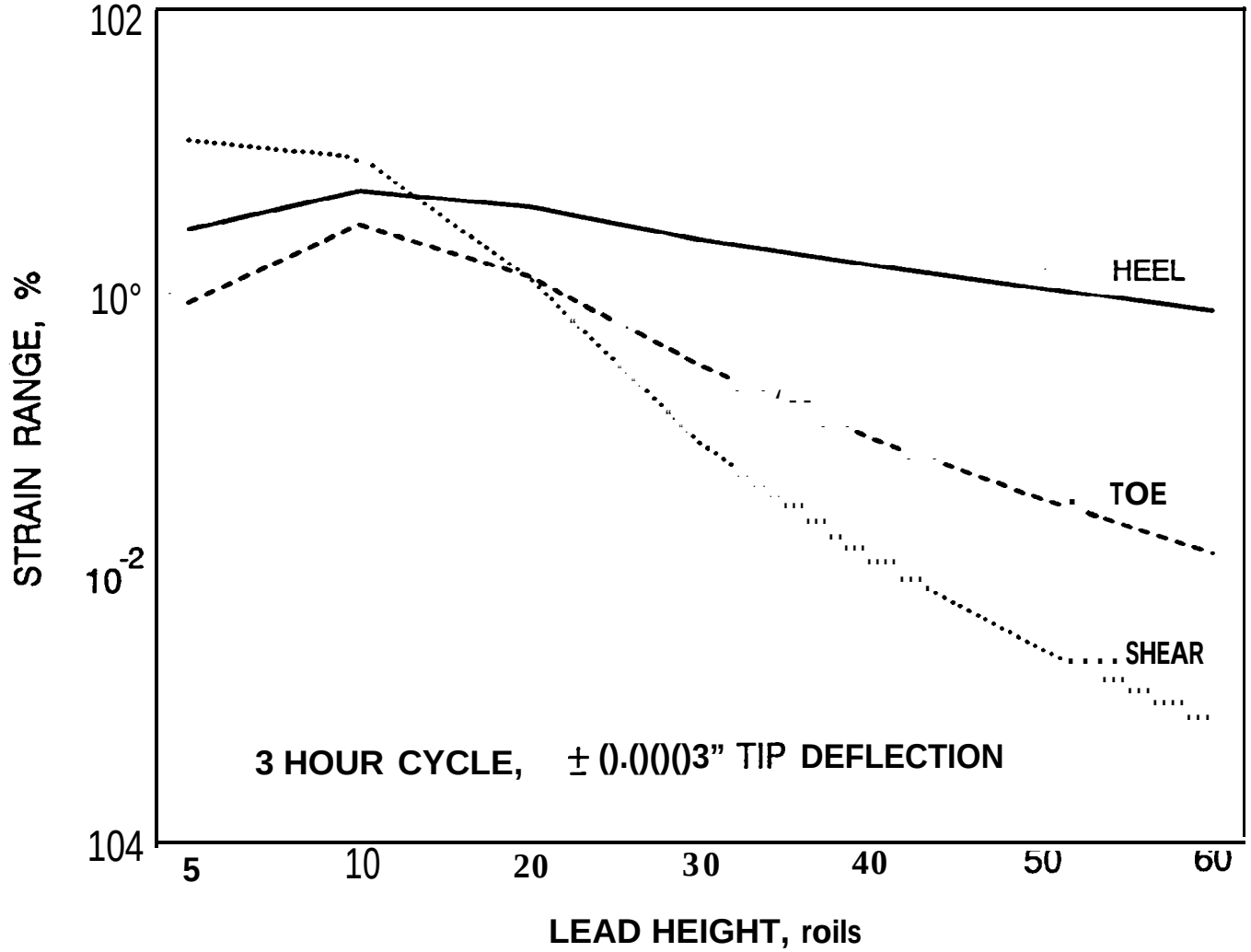

PLOTFILES 378-384

SOD_040

Fig. 16. Dependence of solder strain range on lead deflection range (Δx) and temperature for gull-wing leads with different stiffnesses.

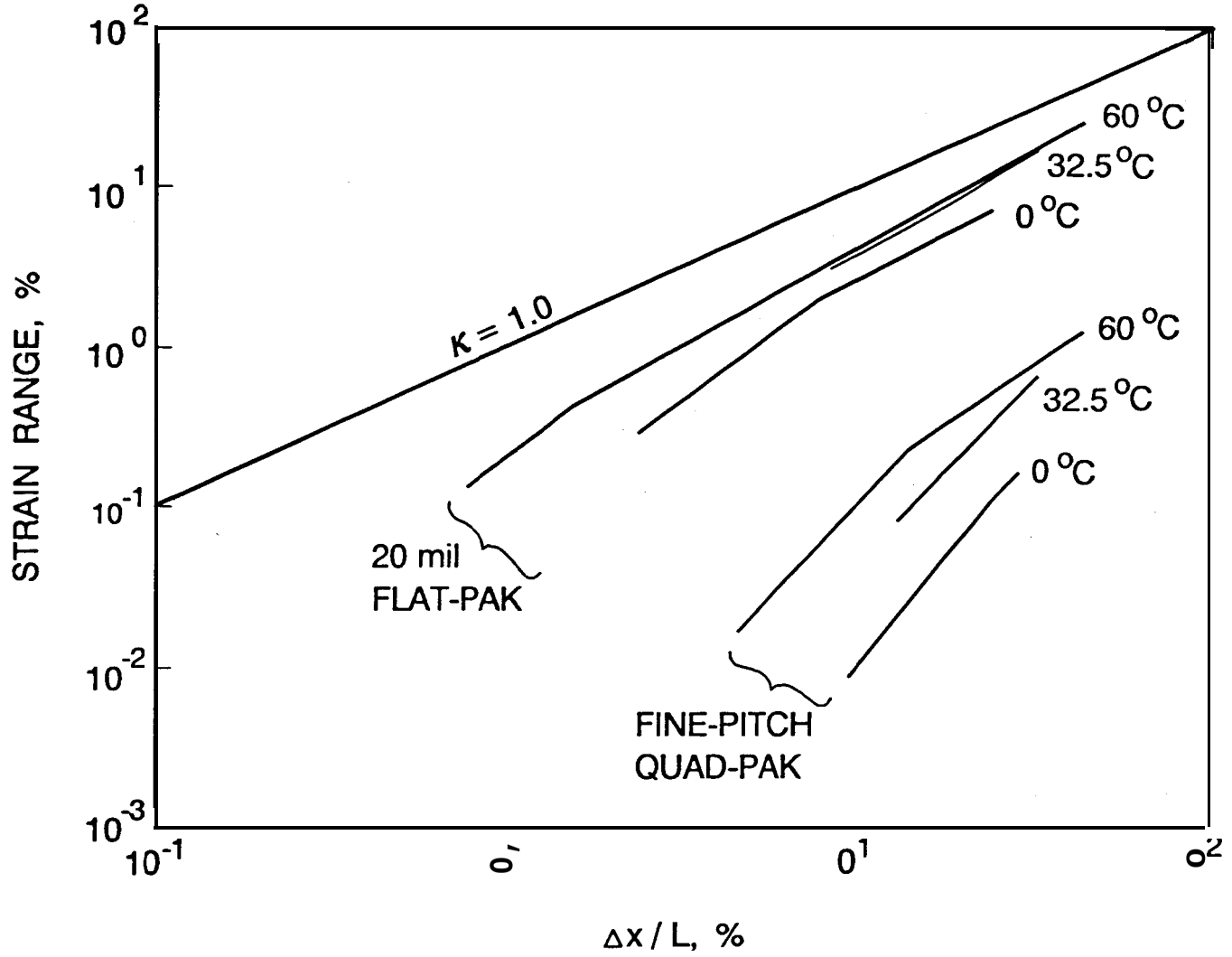

PLOTFILES 582-642, 655-672

SO 04

Fig. 17. Dependence of solder strain range on cyclic frequency for gull-wing leads of different stiffnesses.

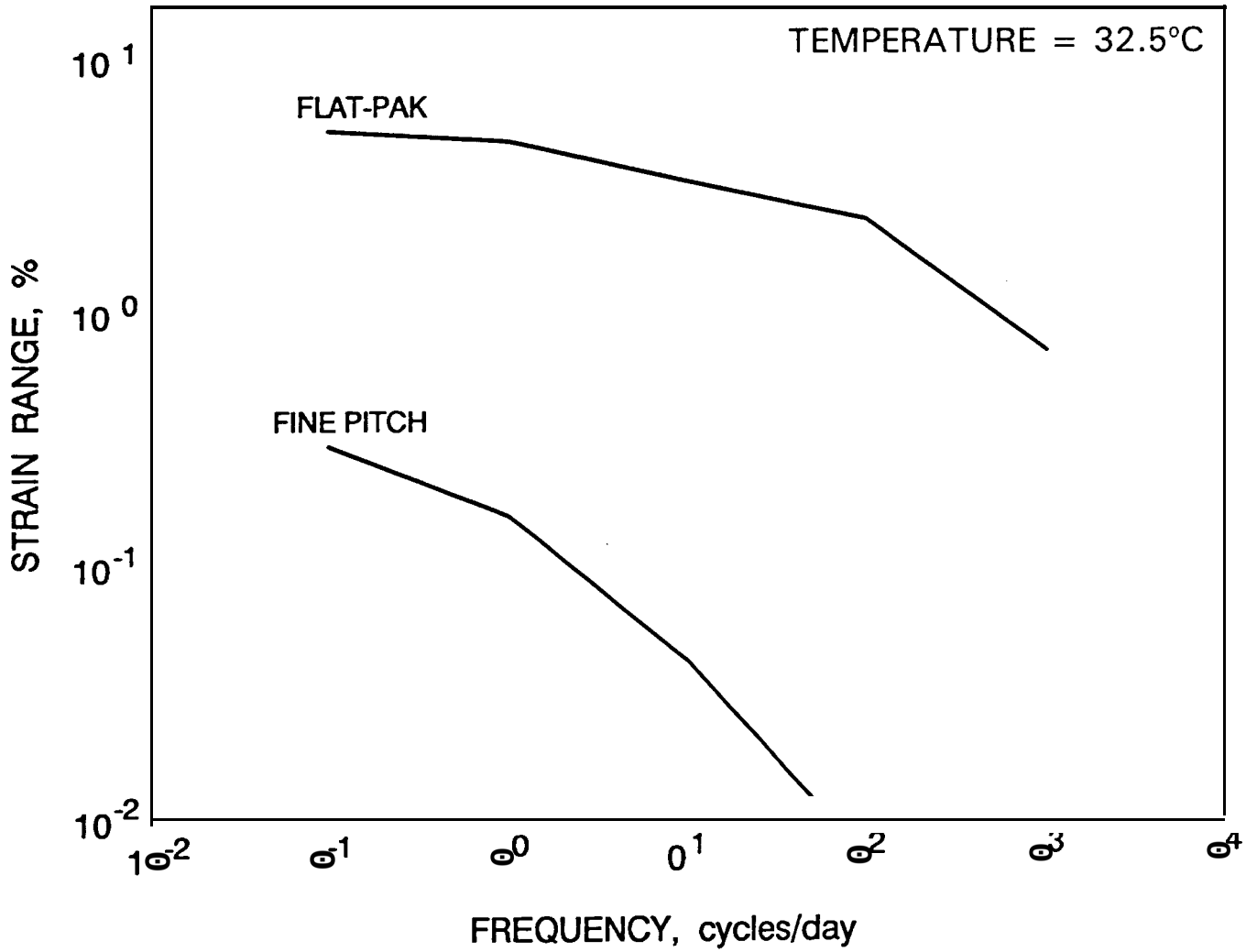

PLOTFILES 673-682 and 645(668)

SOD_043